

Assessment of left ventricular diastolic function with cardiovascular MRI: what radiologists should know

Ricardo Duarte, Gabriel Fernandez-Perez, Nuno Bettencourt, Francisco Sampaio, Diana Miranda, Manuela França, Pedro Portugal

ABSTRACT

Diastolic dysfunction is a common entity and the predominant cause of heart failure in 40%–50% of patients. Diagnosis of diastolic dysfunction is clinically relevant and associated with a poor prognosis. The aim of this essay was to review the pathophysiology and different grades of diastolic dysfunction and to provide an overview on the role of cardiovascular magnetic resonance imaging in the assessment of diastolic function.

Key words: • diastole • heart failure • magnetic resonance imaging

In clinical practice, heart failure (HF), caused by a predominant abnormality in diastolic function, is a common entity and a cause of significant morbidity and mortality. According to the American Heart Association, the prevalence of HF in adults was 5.3 million in 2005, of which almost half had a normal left ventricular (LV) ejection fraction (EF) (1). Diastolic dysfunction occurs when LV relaxation and/or compliance are impaired and is considered an early marker of cardiovascular disease (2). Diastolic HF is a clinical entity, and the diagnosis requires three conditions: the presence of signs or symptoms of HF, normal or slightly abnormal LV systolic function (EF >50%), and demonstration of LV diastolic dysfunction (3). Assessment of diastolic function by cardiovascular magnetic resonance imaging (CMRI) is feasible and could provide a more comprehensive clinical understanding of LV function in addition to a systolic functional assessment. LV diastolic dysfunction occurs in several cardiac and systemic diseases such as hypertension, ischemic heart disease, hypertrophic cardiomyopathy, aortic valve stenosis, and infiltrative cardiomyopathies such as amyloidosis (4).

The purpose of this study was to review the pathophysiology of diastolic dysfunction, to illustrate the different degrees of diastolic dysfunction, and to provide an overview of the role of CMRI in the assessment of diastolic dysfunction.

Physiology of diastole

Diastole represents the portion of the cardiac cycle that begins with isovolumic relaxation and ends with mitral valve (MV) closure, leading to ventricular filling (5).

Diastole can be divided into four phases (Fig. 1):

- 1) Isovolumic relaxation: Relaxation is an energy-dependent process that starts in late systole and ends in mid-diastole. The elastic recoil of the contracted myocardium creates a “suction” mechanism causing the intra-ventricular pressure to decline, while maintaining a virtually constant volume.
- 2) Rapid filling: Pressure continues to decline due to LV relaxation and elastic recoil until it is below the left atrial (LA) pressure so the MV will open, and rapid filling begins. It ends when LV pressure equals LA pressure and is responsible for nearly 70% of LV filling.
- 3) Diastasis: It is the period between rapid filling and atrial contraction, when LA and LV pressures have reached an equilibrium. LV filling continues because of the inertia of pulmonary venous return flow, accounting for <5% of LV filling.
- 4) Atrial contraction: This corresponds to the LA contraction that causes LA pressure to rise above the ventricular pressure; it induces new blood flow into the LV and accounts for nearly 25% of LV filling (4).

From the Departments of Radiology (R.D. ✉ guerra.duarte@gmail.com, D.M., P.P.), and Cardiology (N.B., F.S.), Centro Hospitalar de Vila Nova de Gaia/Espinho, Vila Nova de Gaia, Portugal; the Department of Radiology (G.F.P.), HNS Sonsoles, Avila, Spain; the Department of Radiology (M.F.), Centro Hospitalar do Porto, Porto, Portugal.

Received 15 December 2011; revision requested 21 January 2012; revision received 30 January 2012; accepted 31 January 2012.

Published online 13 July 2012
DOI 10.4261/1305-3825.DIR.5510-11.1

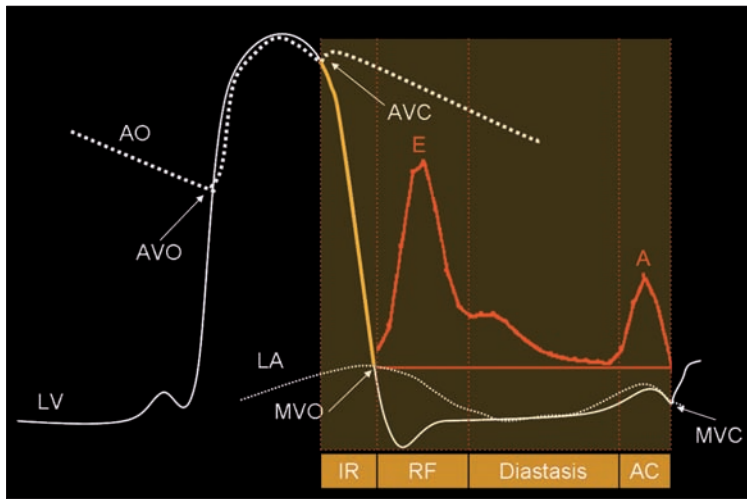


Figure 1. Diagram of the hemodynamic cardiac cycle. The cardiac cycle is broadly divided into systole and diastole. The shaded area shows diastole, which is traditionally divided into four phases: isovolumic relaxation (IR), rapid filling (RF), diastasis, and late ventricular filling or atrial contraction (AC). The relationship between the normal mitral inflow pattern (red line) and the diastolic phases of the cardiac cycle is indicated. AO, aorta; LV, left ventricle; LA, left atrium; AVO, aortic valve opening; MVO, mitral valve opening; AVC, aortic valve closure; MVC, mitral valve closure; E, E wave; A, A wave.

Assessment of diastolic function by CMRI

Clinical methods to assess diastolic function include cardiac catheterization,

single-photon emission computed tomography (SPECT), echocardiography, and CMRI. Although considered the

golden standard, cardiac catheterization with ventriculography is invasive and expensive; therefore not feasible for routine clinical use (6). Echocardiography is the most frequently used method (4). In the past few decades, CMRI has gained an increasing role in evaluating the cardiovascular system and allows for the assessment of diastolic function through several methods (6).

Diastolic time-volume curves

The LV time-volume relationship was the first method used to assess diastolic function by CMRI and is derived from SPECT. The LV time-volume relationship represents relative volume changes throughout the cardiac cycle and therefore may also be used to study LV filling, which is dependent on LV diastolic function. This method requires segmentation of the LV and delineation of the endocardium in all cardiac cycle phases, which is time-consuming in terms of post-processing (Fig. 2); thus, it is rarely used (6, 7).

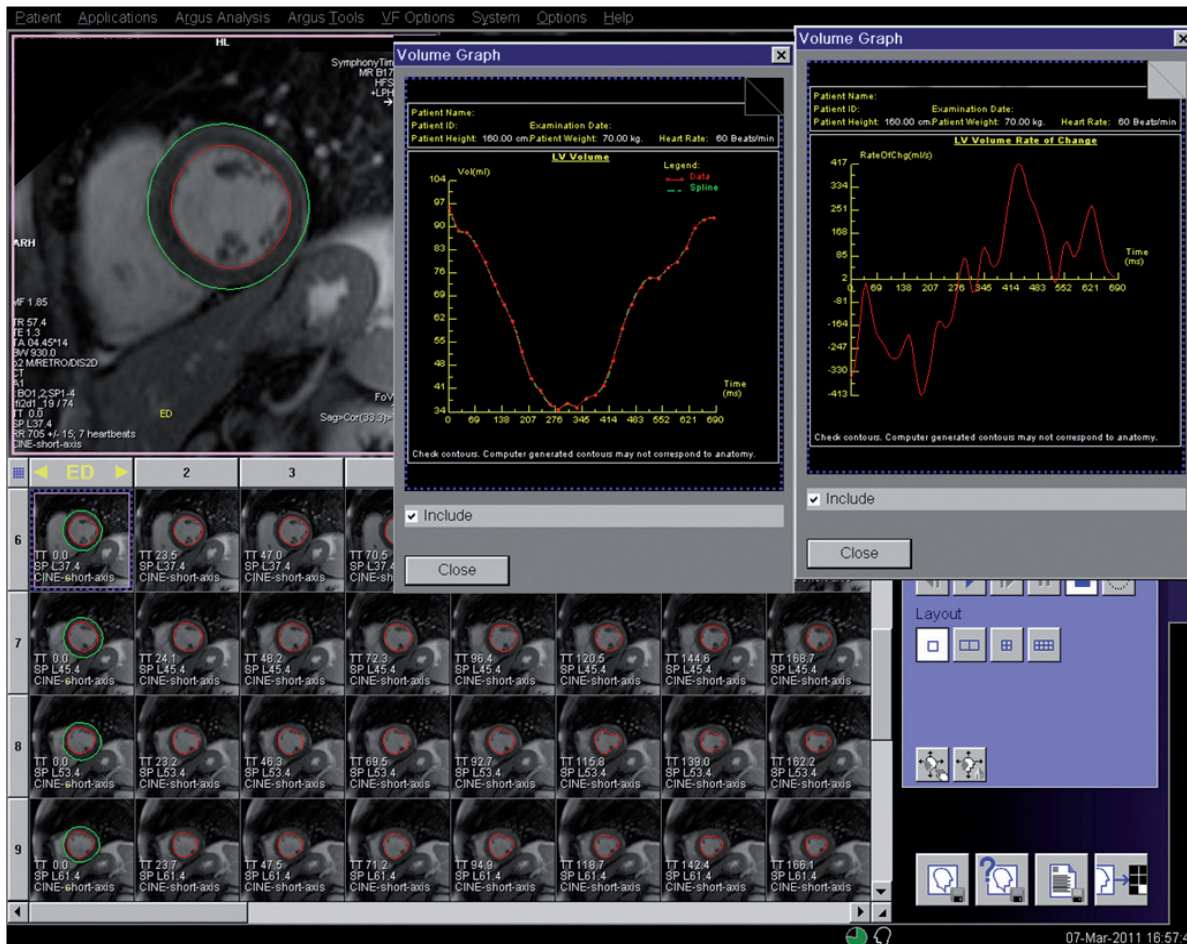


Figure 2. Left ventricular (LV) time-volume curve post-processing and analysis. From the three-dimensional volumetric data obtained with cine sequences on the LV short-axis, the endocardial borders are traced phase by phase for each slice. LV volume curves during the cardiac cycle and the LV filling rate are then produced.

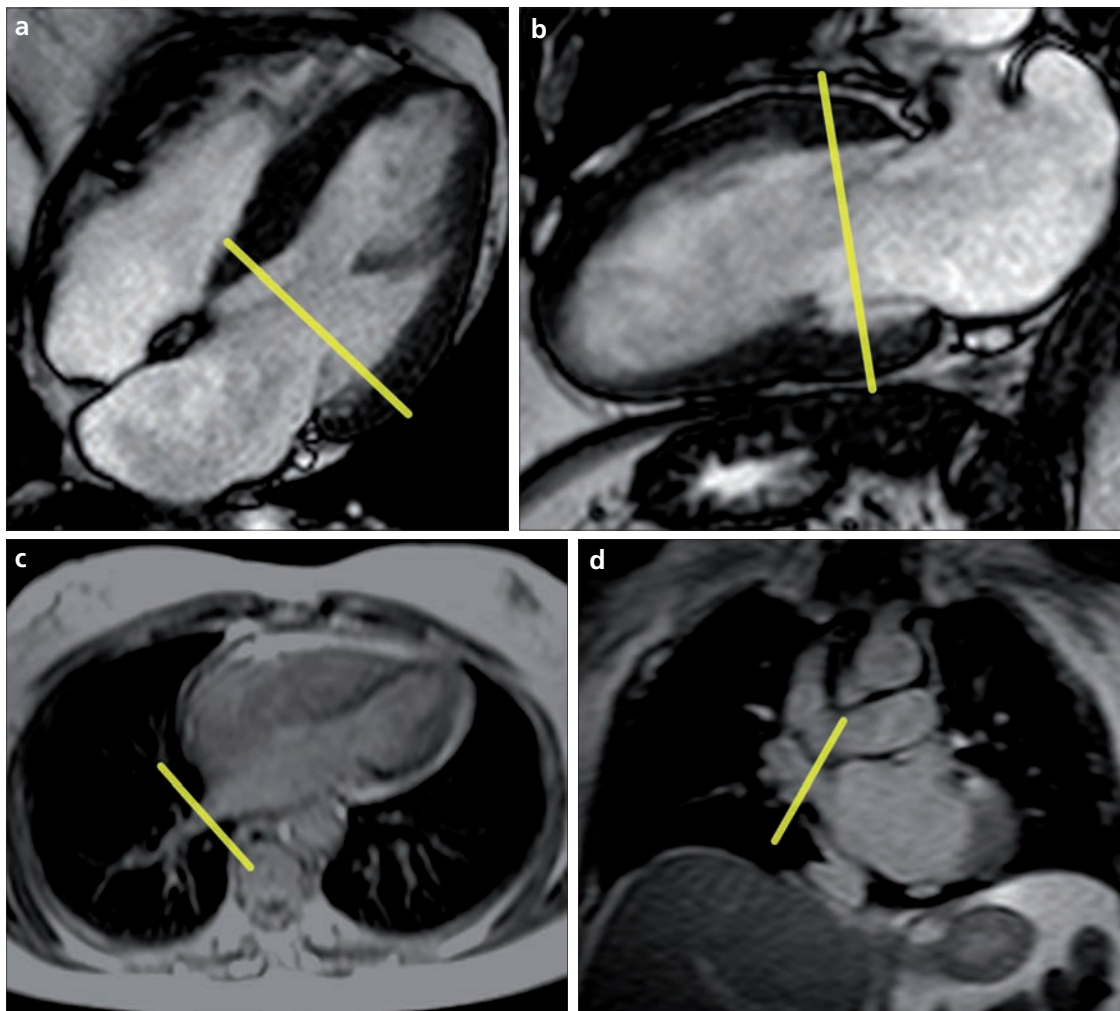


Figure 3. a–d. Mitral inflow and pulmonary venous flow imaging. Cine four-chamber (a) and two-chamber (b) views show the orientation of the acquisition slice for mitral inflow imaging (yellow lines), positioned parallel to the mitral valve (MV) annulus at the MV leaflet tips (through-plane). Axial (c) and coronal (d) surveys show the orientation of the acquisition slice for pulmonary venous flow imaging (yellow lines), positioned 1 cm away from the junction of the right superior pulmonary vein with the left atrium.

Mitral inflow and pulmonary venous flow imaging

Assessment of mitral inflow and pulmonary vein flow by CMRI phase-contrast imaging is based on similar parameters to those obtained by Doppler echocardiography and reflects the LV filling pattern (7–9). Pressure gradients can also be calculated using the modified Bernoulli equation: Pressure gradient (mmHg) = $4V_{\max}^2$ (m/s), where V_{\max} is the peak velocity (10).

The acquisition slice should be positioned at the MV leaflet tips parallel to the mitral annulus (through-plane) for the mitral inflow and at the right superior pulmonary vein perpendicular to the blood flow (through-plane), 1 cm away from the junction with the LA for the pulmonary vein flow (Fig. 3). Phase-contrast images are acquired with retrospective electrocardiogram gating

covering the entire cardiac cycle (40–60 phases per cycle), usually using a velocity encoding of 90–150 cm/s for mitral inflow and 80–100 cm/s for pulmonary vein flow.

Normal mitral inflow pattern

The normal pattern is characterized by an initial ventricular flow (E wave) and late ventricular flow (A wave) (Fig. 4). The E wave is greater than the A wave, as the majority of LV filling occurs during rapid filling, and atrial contraction has a small contribution to LV filling. Consequently, the peak velocity ratio of the E and A waves, called the E/A ratio, is >1 in normal patients.

Normal pulmonary venous flow pattern

The normal pattern is composed of three waveforms: a systolic (S wave)

and a diastolic flow (D wave), usually with similar flow velocities, and a reversed flow (AR wave) at end-diastole (Fig. 5). The S wave corresponds to flow into the LA during ventricular systole. The D wave represents the reduction in LA pressure during rapid filling. The AR wave is due to the atrial contraction.

Valsalva maneuver

The strain phase of the Valsalva maneuver reduces preload and is a simple approach to decrease LA pressure. Therefore, complementary mitral inflow could be performed under the Valsalva maneuver, which in normal patients will show proportional reductions in both E and A waves velocities, and the E/A ratio will remain >1. Clinically, this maneuver can be used to unmask a pseudonormal

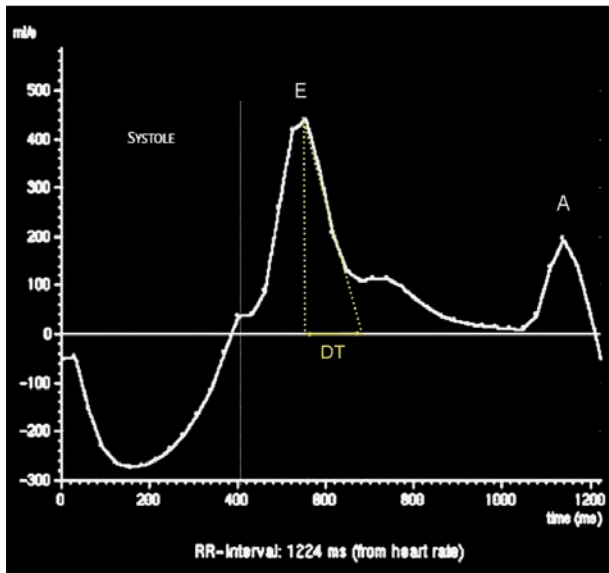


Figure 4. Normal mitral inflow pattern. The first negative peak is due to LV outflow during systole. The first positive peak at the beginning of diastole (E wave) corresponds to rapid filling, and the second positive peak corresponds to atrial contraction (A wave). E wave deceleration time was measured according to the method described by Gatehouse et al. (10). E, E wave; A, A wave; DT, deceleration time.

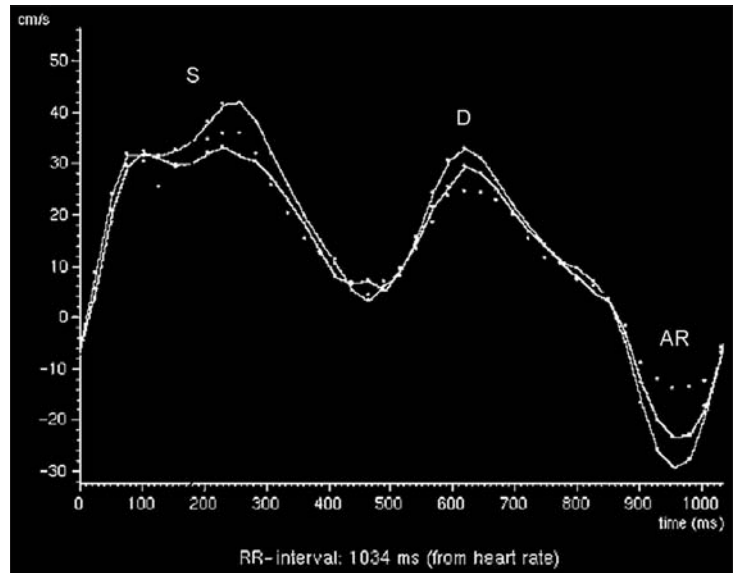


Figure 5. Normal pulmonary venous flow pattern. The S wave occurs during ventricular systole and has one or two peaks; the first systolic peak (S1) is caused by the reduction of LA pressure due to LA relaxation and longitudinal LV shortening, and the second systolic peak (S2) reflects right ventricle stroke volume and atrial compliance. The D wave occurs during diastole and reflects ventricular filling. The A wave, which has an opposite direction to the other two waves, occurs during atrial contraction and reflects ventricular compliance. S, S wave; D, D wave; AR, AR wave.

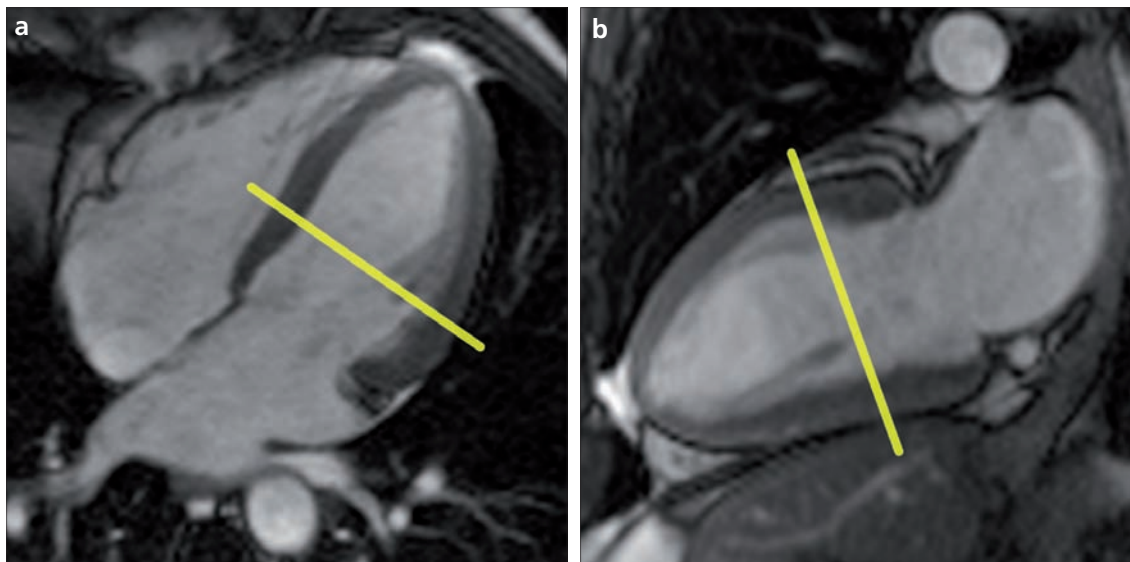


Figure 6. a, b. Myocardial tissue imaging. Cine four-chamber (a) and two-chamber (b) views show the orientation of the acquisition slice (yellow lines), positioned parallel to the MV annulus at two-thirds of the LV long-axis.

pattern and distinguish the restrictive reversible pattern from the irreversible pattern (11).

LA size

Long-standing exposure of the LA to increased LV filling pressure results in increased LA wall tension and ultimately in dilatation. Thus, LA size is a structural rather than functional parameter that reflects elevated LV filling pressure and considered a useful marker for chronic diastolic dysfunction.

Additionally, increased LA size is an important predictor of adverse cardiovascular events such as atrial fibrillation, ischemic stroke, and HF survival (7). LA quantification techniques rely on measurements of LA area or volume.

CMRI research techniques

Myocardial tissue imaging

A diastolic functional evaluation should include a study of mitral annular velocity or so-called myocardial

tissue imaging (MTI), which reflects the shortening and lengthening of the myocardium and provides an index of LV relaxation that is not affected by LA pressure (9). MTI can be assessed by phase-contrast images using a velocity encoding of 20–30 cm/s. Acquisition slices should be positioned parallel to the MV annulus at two-thirds of the LV long-axis (Fig. 6) (12).

The normal MTI pattern is composed of three basic waveforms: systolic myocardial motion, early diastolic

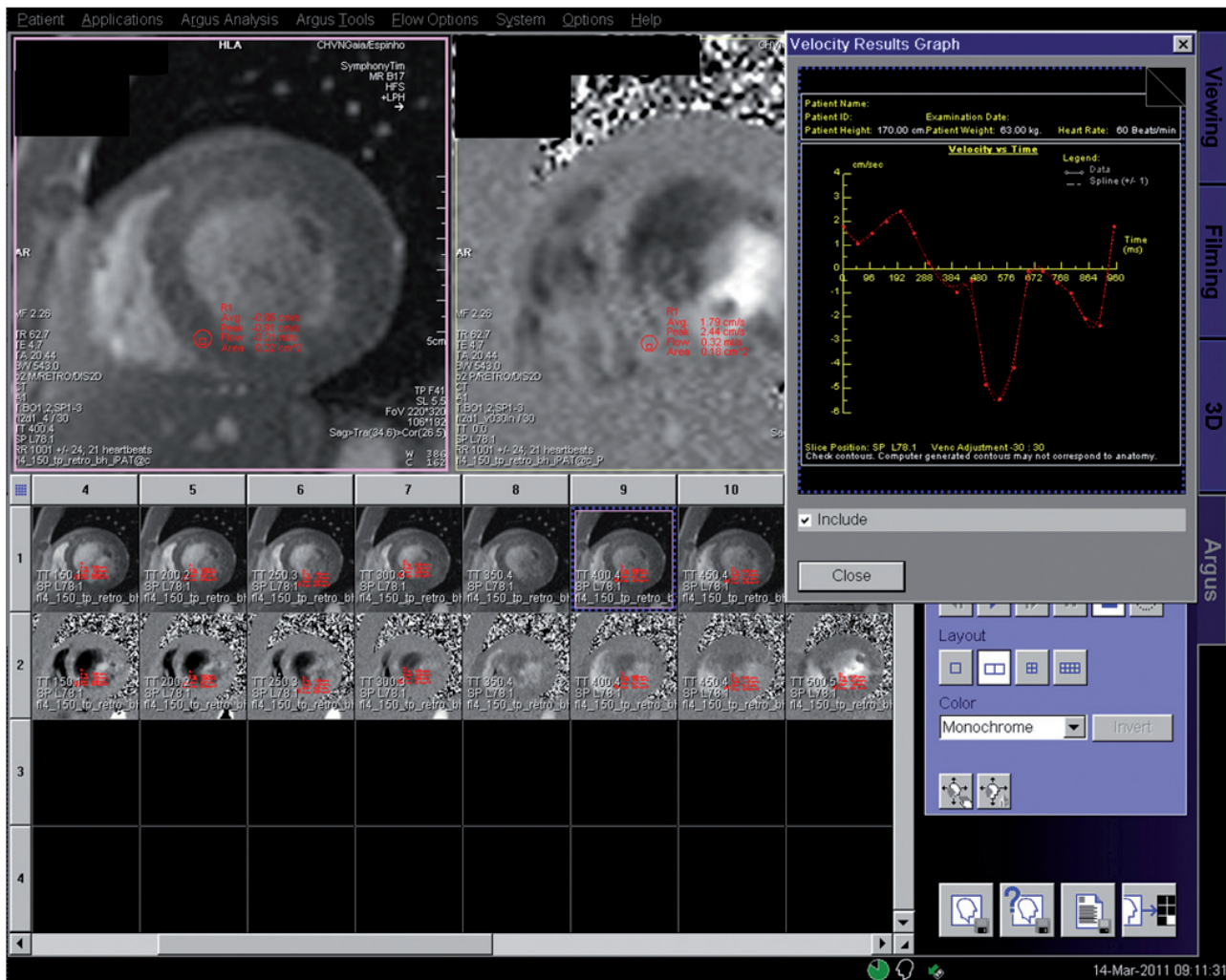


Figure 7. Illustration of myocardial tissue imaging post-processing and analysis. The data analysis should be performed at the inferoseptal mitral annulus region, which shows better agreement with echocardiography. The normal myocardial tissue imaging pattern is composed of three waves: the Sa wave, which corresponds to ventricular systole and is the only wave above baseline; the Ea wave, which is the first wave below the baseline that corresponds to rapid filling and is related to the LV velocity of relaxation; and the Aa wave, which is the second wave below the baseline and represents passive myocardial distension caused by atrial contraction.

mitral annulus motion (Ea), and late diastolic mitral annulus motion (Fig. 7). The Ea wave corresponds to rapid filling and its peak velocity reflects the velocity of early myocardial relaxation as the mitral annulus ascends away from the apex. LV filling pressures can be estimated using the peak velocity ratio of the E and Ea waves, called the E/Ea ratio, which integrates the early filling parameters of mitral inflow with MTI. Thus, an E/Ea ratio ≤ 8 usually predicts normal filling pressures and an E/Ea ratio >15 foretells elevated filling pressures. When the E/Ea ratio is 8–15, the use of additional parameters (e.g., Valsalva maneuver and/or pulmonary vein flow) to correctly classify LV diastolic function is recommended.

Myocardial tagging

CMRI can label (“tag”) the myocardium, which allows for easy visualization of systolic and diastolic myocardial deformations. These deformations are commonly measured using units of strain (%S) or torsion (degrees). Therefore, CMRI tagging provides an accurate analysis of LV torsion recovery and strain rate recovery that directly reflects the mechanisms of myocardial diastolic relaxation (9). The diastolic torsion recovery rate is extended in patients with LV impaired diastolic function.

³¹P-MR spectroscopy

³¹P-MR spectroscopy is currently only available for research and allows measurement of the myocardial

phosphocreatine/adenosine triphosphate ratio, which reflects myocardial energy status (6).

Diastolic dysfunction grading

Diastolic dysfunction can be classified into four grades (5). Diastolic parameters with progressively worsening diastolic function are as follows (Fig. 8):

Grade I

In grade I, an impaired relaxation occurs, so mitral inflow velocity is lower at the beginning of diastole (reduced E wave), which is partially compensated for by increased flow during atrial contraction (increased A wave); this leads to a reverse E/A ratio and an increase in deceleration time (Fig. 9a). At this

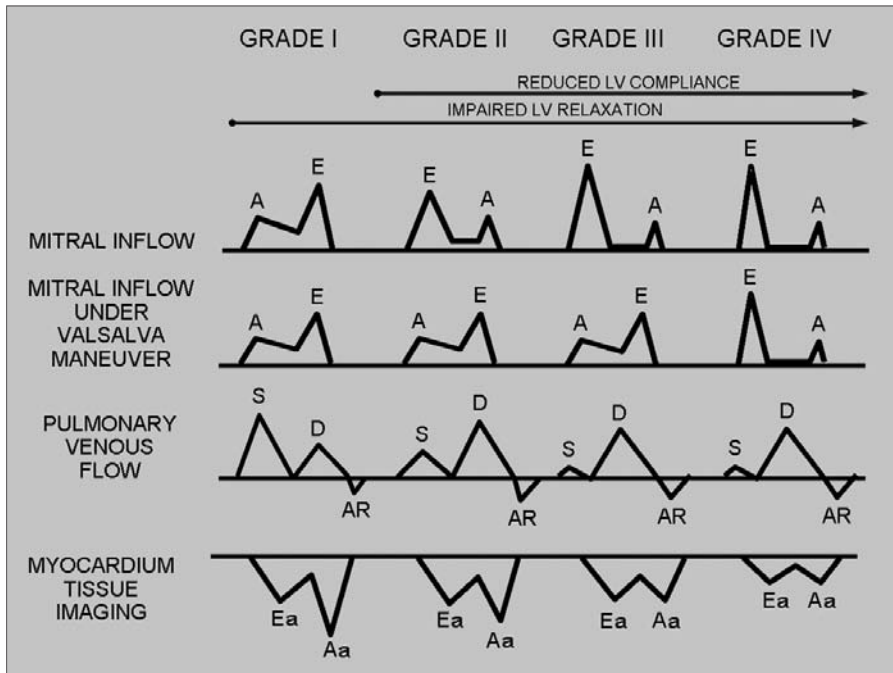


Figure 8. Schematic representation of grading for diastolic dysfunction. Mitral inflow, pulmonary venous flow, and myocardium tissue imaging patterns are shown in the presence of worsening diastolic dysfunction. LV, left ventricle; E, E wave; A, A wave; S, S wave; D, D wave; AR, AR wave; Ea, Ea wave; Aa, Aa wave.

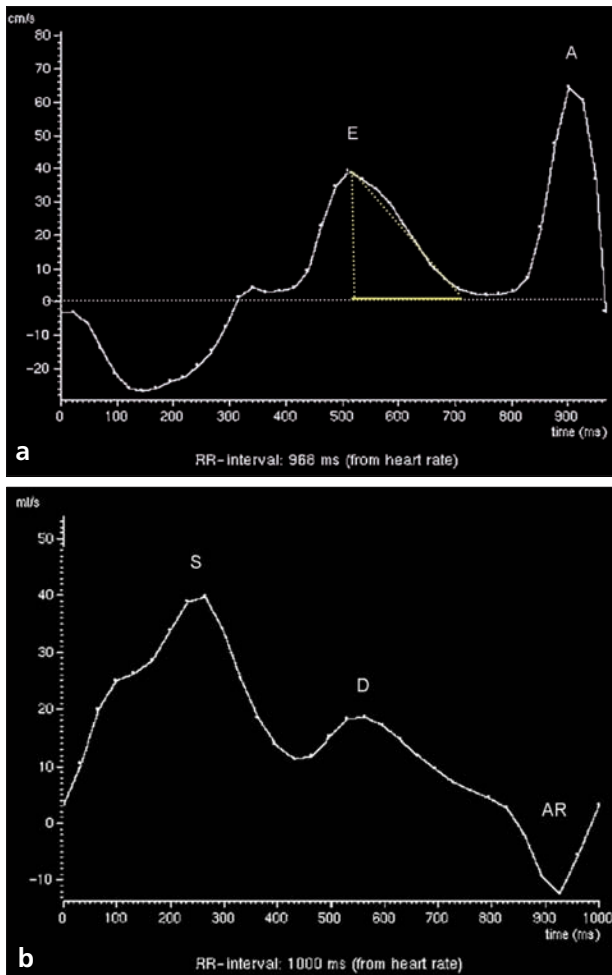


Figure 9. a, b. Impaired relaxation in a 63-year-old asymptomatic woman with preserved LV systolic function and long-standing history of hypertension. Mitral inflow (a) shows an E wave < A wave with an E/A ratio < 1 and an increased deceleration time. Pulmonary venous flow (b) demonstrates a decreased D wave (S wave > D wave). E, E wave; A, A wave; S, S wave; D, D wave; AR, AR wave.

stage, pulmonary vein flow shows a decrease in diastolic flow (decreased D wave) (Fig. 9).

Grade II

A progressive increase in LV pressure at the end of diastole reduces the contribution of atrial contraction to LV filling, and most of the LV filling occurs at the beginning of diastole. This results in a mitral inflow pattern similar to normal, as the E wave is higher than the A wave and the E/A ratio > 1. Therefore, this state is considered pseudonormal (Fig. 10). The differential diagnosis between grade II and the normal pattern can be made by MTI. Alternatively, the Valsalva maneuver and pulmonary vein flow can be used, with pulmonary vein flow typically showing decreased systolic flow (S < D).

Grades III and IV

Finally, severe impairment of LV compliance and relaxation results in increased LA pressure and LV diastolic filling pressures. The markedly elevated LA pressure leads to an earlier opening of the MV (decreased isovolumic relaxation time), raising the atrioventricular pressure gradient and increasing the velocity of early diastolic filling (increased E wave). As a result, early ventricular filling stops abruptly due to the severe impairment of LV relaxation and compliance, resulting in reduced deceleration time. Furthermore, the atrial contribution (reduced A wave) is even more attenuated as a result of the rapid early elevation in LV pressure (E >> A; E/A ratio > 1.5). Pulmonary vein flow shows decreased systolic flow (S << D) due to a decrease in the pressure gradient between the pulmonary veins and LA; the AR wave is also usually wider (≥ 30 ms). Moreover, the E/Ea ratio is > 15. The Valsalva maneuver can be used to distinguish the reversible from the irreversible restrictive pattern: if the mitral inflow pattern modifies to a grade I or II under this maneuver, the restrictive pattern is considered reversible (grade III). If not, the restrictive pattern is considered irreversible (grade IV) (Fig. 11).

A restrictive pattern is associated with a poor prognosis, as it is characteristic of infiltrative cardiomyopathies, dilated cardiomyopathies with poor systolic function, and pericardial diseases (Fig. 12).

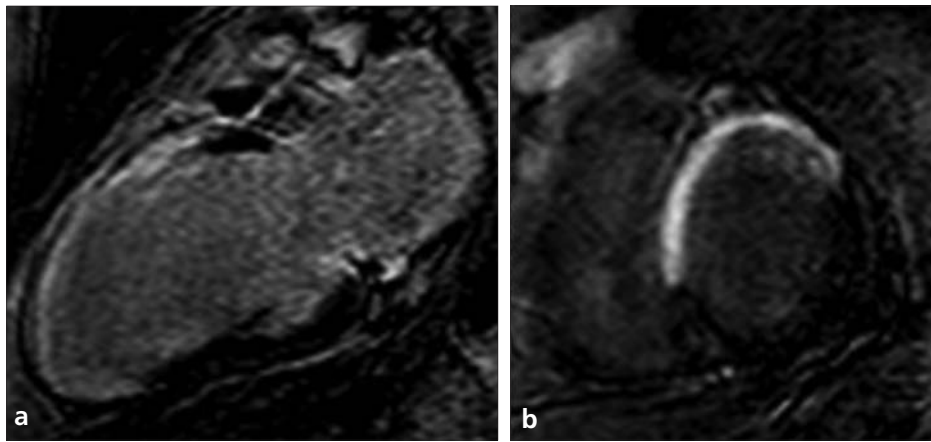


Figure 10. a–e. Pseudonormal pattern in a 52-year-old man with ischemic heart disease and LV ejection fraction of 29%. Late enhancement images in short-axis (a) and two-chamber (b) views show an anteroseptal scar from a previous extensive anterior myocardial infarct. Mitral inflow analysis (c) revealed a pseudonormal pattern (E wave > A wave; E/A ratio >1) that reverted to an impaired relaxation pattern (d) under the Valsalva maneuver (E wave < A wave; E/A ratio <1). Pulmonary venous flow (e) demonstrates a D wave greater than the S wave, reflecting an increase in the LA pressure. E, E wave; A, A wave; S, S wave; D, D wave; AR, AR wave.

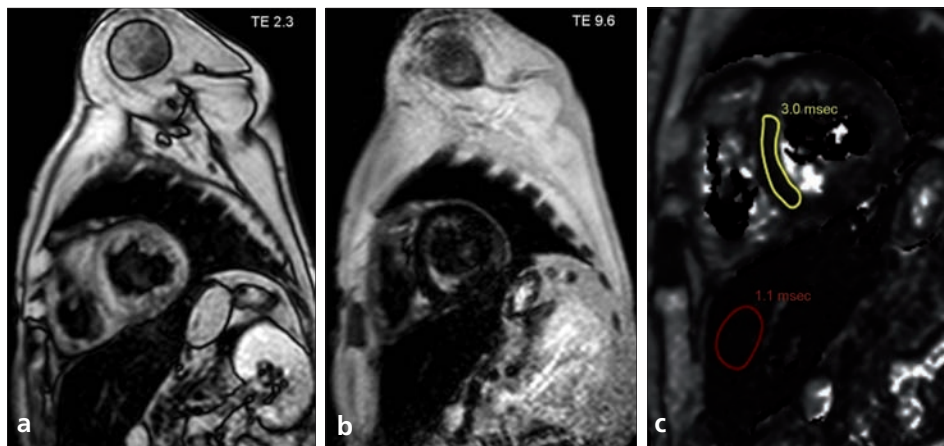
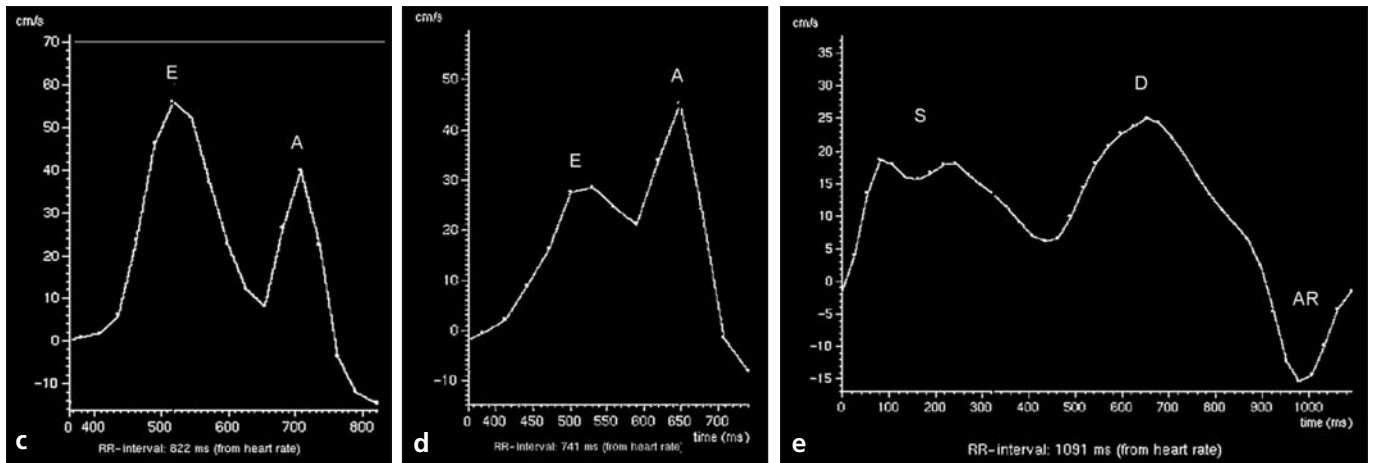
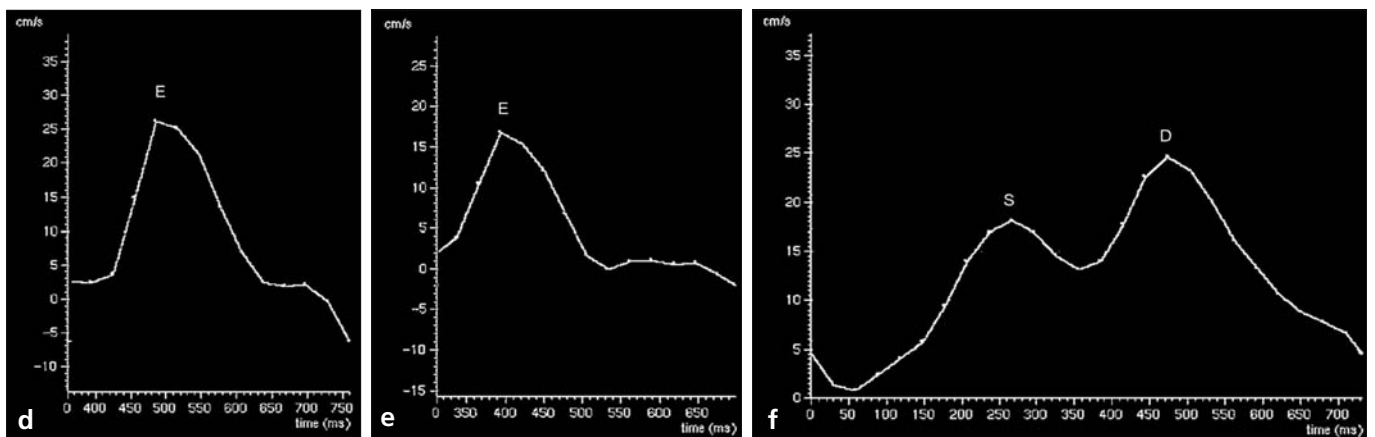


Figure 11. a–f. Irreversible restrictive pattern in a 33-year-old man with thalassemia major and preserved LV ejection fraction of 58%. Mid-myocardial short-axis gradient-echo images (a, b) of the heart and liver acquired with increasing echo time (TE) show a reduction in the myocardial and liver signals due to iron overload. CMRI of the myocardium and liver T2* (c) shows a short T2*, which reflects heavy heart and liver iron overload (normal T2* >20 ms). Mitral inflow analysis (d) revealed a restrictive pattern (increased E and absent A waves), practically unchangeable under the Valsalva maneuver (e). Pulmonary venous flow (f) demonstrated a prominent D wave. E, E wave; S, S wave; D, D wave.



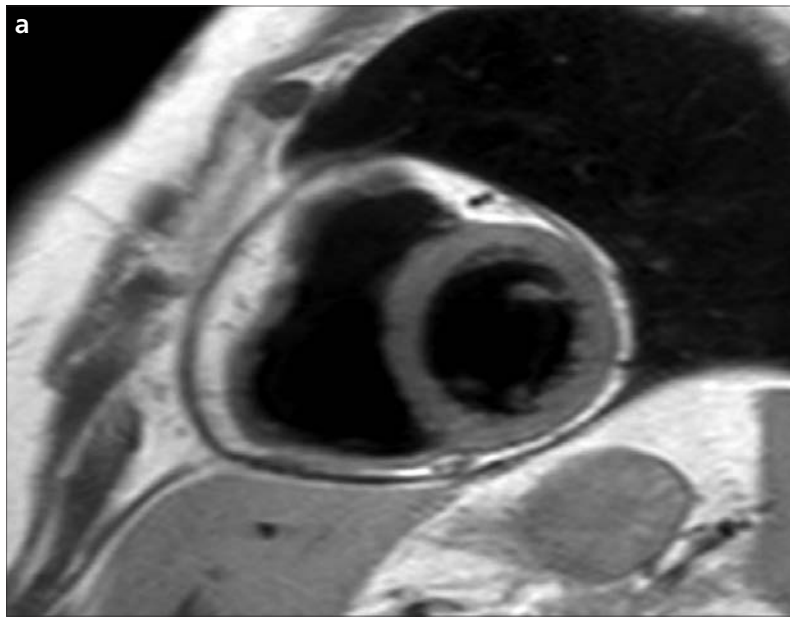
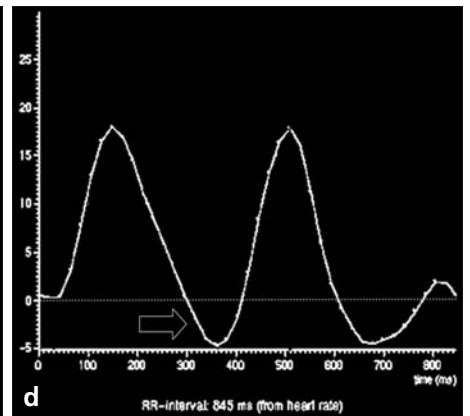
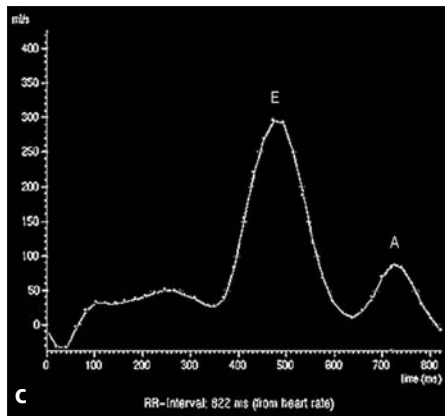
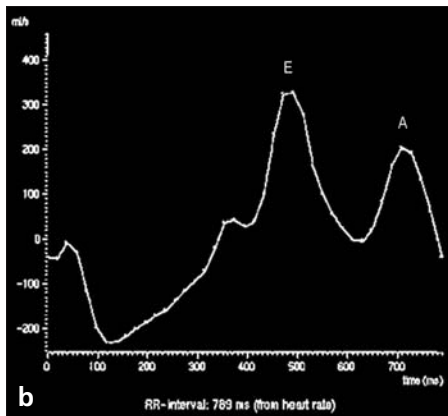


Figure 12. a–d. Constrictive pericarditis. Mid-myocardial short-axis T1-weighted image (a) shows thickened pericardium. Constrictive pericarditis is characterized by dissociation of intra-thoracic and intra-cardiac pressure, which leads to an increase in diastolic driving pressure into the LV with expiration (b) and a decrease with inspiration (c). As a result, mitral inflow shows marked respiratory changes at the beginning of diastole (E wave). Inferior vena cava flow (d) shows reversal of diastolic flow (arrow) during expiration, which is also characteristic. E, E wave; A, A wave.



Conclusion

Diastolic dysfunction is a common clinical condition, being the predominant cause of HF in 40%–50% of patients. Global and regional diastolic function assessments by CMRI are feasible. Moreover, the unique features of CMRI, such as CMRI tagging, which can assess the diastolic recoil properties and ^{31}P -MR spectroscopy, which can measure myocardial energy status, provide insights into the mechanism of diastolic dysfunction not fully available with other modalities.

Conflict of interest disclosure

The authors declared no conflicts of interest.

References

- Rosamond W, Flegal K, Furie K, et al. Heart disease and stroke statistics 2008 update: a report from the American Heart Association Statistics Committee and Stroke Statistics Subcommittee. *Circulation* 2008; 29:25–146.
- Galderisi M. Diastolic dysfunction and diastolic heart failure: diagnostic, prognostic and therapeutic aspects. *Cardiovasc Ultrasound* 2005; 3:9.
- Paulus WJ, Tschöpe C, Sanderson JE, et al. How to diagnose diastolic heart failure: a consensus statement on the diagnosis of heart failure with normal left ventricular ejection fraction by the Heart Failure and Echocardiography Associations of the European Society of Cardiology. *Eur Heart J* 2007; 28:2539–2550.
- Zile MR, Brutsaert DL. New concepts in diastolic dysfunction and diastolic heart failure: Part I: diagnosis, prognosis, and measurements of diastolic function. *Circulation* 2002; 105:1387–1393.
- Mandinov L, Eberli FR, Seiler C, Hess OM. Diastolic heart failure. *Cardiovasc Res* 2000; 45:813–825.
- Rathi VK, Biederman RW. Expanding role of cardiovascular magnetic resonance in left and right ventricular diastolic function. *Heart Fail Clin* 2009; 5:421–435.
- Caudron J, Fares J, Bauer F, Dacher JN. Evaluation of left ventricular diastolic function with cardiac MR imaging. *Radiographics* 2011; 31:239–259.
- Paelinck BP, Lamb HJ, Bax JJ, Van der Wall EE, de Roos A. Assessment of diastolic function by cardiovascular magnetic resonance. *Am Heart J* 2002; 144:198–205.
- Rathi VK, Doyle M, Yamrozik J, et al. Routine evaluation of left ventricular diastolic function by cardiovascular magnetic resonance: a practical approach. *J Cardiovasc Magn Reson* 2008; 10:36.
- Gatehouse PD, Keegan J, Crowe LA, et al. Applications of phase-contrast flow and velocity imaging in cardiovascular MRI. *Eur Radiol* 2005; 15:2172–2184.
- Dumesnil JG, Gaudreault G, Honos GN, Kingma JG Jr. Use of Valsalva maneuver to unmask left ventricular diastolic function abnormalities by Doppler echocardiography in patients with coronary artery disease or systemic hypertension. *Am J Cardiol* 1991; 68:515–519.
- Paelinck BP, de Roos A, Bax JJ, et al. Feasibility of tissue magnetic resonance imaging: a pilot study in comparison with tissue Doppler imaging and invasive measurement. *J Am Coll Cardiol* 2005; 45:1109–1116.